JOURNAL OF GEOPHYSICAL RESEARCH, VOL. 106, NO. A3, PAGES 3665-3683, MARCH 1, 2001

Detection of small comets with a ground-based telescope

L. A. Frank and J. B. Sigwarth
Department of Physics and Astronomy, University of Iowa, Iowa City

Abstract. The Iowa Robotic Observatory (IRO) located in the Sonoran desert near Sonoita, Arizona, was used for an optical search for small comets in the vicinity of Earth during the period October 1998 through May 1999. The previous reports of detection of the small comets with an optical telescope were based on the search with the Spacewatch Telescope during November 1987, January 1988, and April 1988. The searches with both of these telescopes required that their fields of view be moved in a special manner across the celestial sphere in order to maximize the dwell times of the comet images on a small set of pixels of the telescopes' array detectors. There were sightings of nine small comets in the set of 1500 usable images which were gained with the IRO. The possibility that these events were spurious owing to random fluctuations of the responses in the sensors was eliminated in two different ways. The first method was the use of a shutter to provide either two or three trails for the same small comet. In the two-trail mode, no events were seen with three trails, and for the three-trail mode, no events were seen with two trails. The second assurance that the trails were not due to noise was provided by a rigorous determination of the signals S and signal-to-noise ratios (S/N) in the trails due to random statistical fluctuations, or "random trails," and the subsequent comparison with these parameters for the small-comet sightings. The diameter of the primary mirror of the IRO is significantly smaller than that of the Spacewatch Telescope, and thus the uncertainties in the number densities of the small comets are greater with the IRO. However, within a factor of 2 or 3, the average number densities of small comets detected with the IRO are similar to those observed previously with the Spacewatch Telescope, that is, about 10^{-18} /m^3.

1. Introduction

Fourteen years ago, *Frank et al.* [1986a, b] reported the existence of transient decreases of far-ultraviolet intensities in Earth's dayglow as seen in global images with a camera on the Dynamics Explorer 1 spacecraft. The maximum diameters of these "atmospheric holes" were in the range of 100 km, and their durations were about 1 to 2 min. These atmospheric holes were interpreted in terms of the disruption of small comets above our atmosphere and their subsequent vaporization due to exposure of their water snows to sunlight before impact with the atmosphere. Water vapor is an efficient absorber of the far-ultraviolet dayglow, and tens of tons of this vapor are sufficient to occlude the dayglow over an area equal to that of an atmospheric hole. Whereas the scientific community was willing to accept the impacts of several tens, perhaps hundreds of small comets into the atmosphere during the course of a year, the actual rate of atmospheric holes was an unsettling 10 million per year. Understandably, a large number of scientists concluded that the proposed existence of such a large small-comet population was inconsistent with the current wisdom concerning the Earth and the Moon. These arguments against the existence of the small comets are summarized by *Dessler* [1991]. The responses to each of these arguments are offered by *Frank and Sigwarth* [1993]. It is not our purpose here to review these papers but to address the direct optical searches for these small comets.

The first telescopic search for the small comets at visible wavelengths employed the Spacewatch Telescope at Kitt Peak National Observatory [*Yeates,* 1989]. A special operating mode of the telescope was used which moved its field of view in such a manner as to lock onto the stream of small comets as they passed by Earth in their prograde trajectories near the ecliptic plane. This became known as "skeet shooting" of the small comets. A range for this search which was compatible with the capabilities of the telescope had to be chosen, since larger ranges provided greater search vol-

Paper number 2000JA000054.
0148-0227/01/2000JA000054$09.00

umes. This range was 137,000 km from the telescope's position. The search was successful and the apparent brightnesses of the objects were in the range of 18.2^m to 19.0^m. Such brightnesses can be expected for small comets with diameters in the range of 5 to 10 m surrounded with dark carbon-based mantles. The primary criticism of these detections was the fact that only one image of an individual comet trail was taken. Yeates subsequently returned to the Spacewatch Telescope and successfully obtained two consecutive images of the same small comet [*Sigwarth,* 1989; *Frank et al.,* 1990].

Further efforts for direct detection of the small comets did not occur until the launch of the Polar spacecraft in 1996. Atmospheric holes were again detected in the images of the far-ultraviolet dayglow [*Frank and Sigwarth,* 1999] at about the same global infall rate as that observed with Dynamics Explorer 1, but with much different types of cameras. Also there were two independent optical detections with the cameras on board the Polar spacecraft which corroborate the existence of the small comets in the vicinity of Earth. The first is the discovery of bright trails of atomic oxygen emissions at ultraviolet wavelengths of 130.4 nm from some of the small comets which are disrupted at high altitudes above the atmosphere [*Frank and Sigwarth,* 1997a]. To our knowledge, there are no other spacecraft cameras which are capable of searching the sky for these trails. The second optical detections are the trails due to OH emissions at 308.5 nm with another camera for visible wavelengths. These images are taken as the cometary water clouds are impacting the atmosphere [*Frank and Sigwarth,* 1997b]. These OH emissions are the standard proxy for water in large comets such as Comet Hale-Bopp, which was also viewed by this Polar camera. The intensities of the OH emissions from the small-comet water clouds yield total masses for the small comets which are in the same range as those inferred from the dimensions of the atmospheric holes.

The purpose of our present paper is to report the further confirmation of the presence of small comets in the vicinity of Earth with optical detections with a small ground-based telescope located near Sonoita, Arizona.

2. Description of the Telescope

The Iowa Robotic Observatory (IRO) is equipped with Ritchey-Chretien optics with a Nasmyth focus. The primary mirror diameter is 0.5 m. The telescope mount is an azimuth-elevation design with friction wheel drives. Both of these axes are driven with stepper motors and harmonic gear reducers. This design allows motion of the telescope's field of view which is fully flexible and controlled by associated computer software.

The telescope is mounted in a building which is equipped with a roll-off roof for viewing the sky. Although this design is inexpensive in relation to the costs of the usual dome, the telescope is considerably more exposed to winds which can cause substantial oscillatory motions of the telescope pointing. The telescope is located at the Winer Mobile Observatory about 3 miles SSE of Sonoita, Arizona, in the high-altitude Sonoran desert. The sky glow at this position is significantly brighter than that for the mountain location of the Kitt Peak National Observatories but is adequate for the small-comet search during the darkest nights and when moonlight is not present. The primary use of the telescope is for student projects for their astronomy course activities.

The telescope's camera is an Apogee Instruments model AP-8 and is equipped with a SITe type Si-503a charge-coupled device (CCD). The peak quantum efficiency is ~90% with good blue sensitivity. The read noise of the electronics is ~15 electrons, and the dark current is <1 electron/pixel/s. The format of the CCD is 1024 × 1024 pixels (picture elements). The angular dimension of the square field of view for a single pixel is 1.23 arcsec. Thus the corresponding full field of view is 0.35° × 0.35°, or ~0.12 deg^2. For comparison, the field of view of the Spacewatch Telescope was 0.04 deg^2 during the previous small-comet search.

Calibrations of the IRO sensitivity with a clear filter find that the responses to stars with similar spectral characteristics as those for our Sun were 2200 dn (digitization numbers) for visual magnitude $V = 16.5^m$ in an integration time of 30 s. One digitization number corresponds to 5 electrons in a CCD pixel. This is the sensitivity used for the sightings of small comets reported in this paper. This calibration was checked by using the extensive calibrations for the Spacewatch Telescope [*Sigwarth,* 1989]. The major factors in converting the Spacewatch sensitivity into that for the IRO were the larger ratio of the primary mirror areas, 3.3, and smaller quantum efficiencies, (75%)/(85%), for the Spacewatch Telescope and the latter's digitization number corresponding to 25 pixel electrons per dn. The accuracy of the IRO calibration is considered to be ±25% in dn for a given visual magnitude, or $\delta V = \pm 0.2^m$. Such accuracies are adequate for the present small-comet search, the primary purpose of which is to confirm the previous Spacewatch optical detections of the small comets.

3. Design of the Search Mode

A diagram of the search mode for detection of the small comets is shown in Figure 1. The small comets are small, dark objects which are moving in a prograde stream with speeds of about 10 km/s in the Earth's reference system and with orbits generally parallel to the ecliptic plane [*Frank et al.,* 1986b; *Frank and Sigwarth,* 1993]. A telescope with field of view staring in a fixed direction on the celestial sphere, i.e., the usual mode of observing,

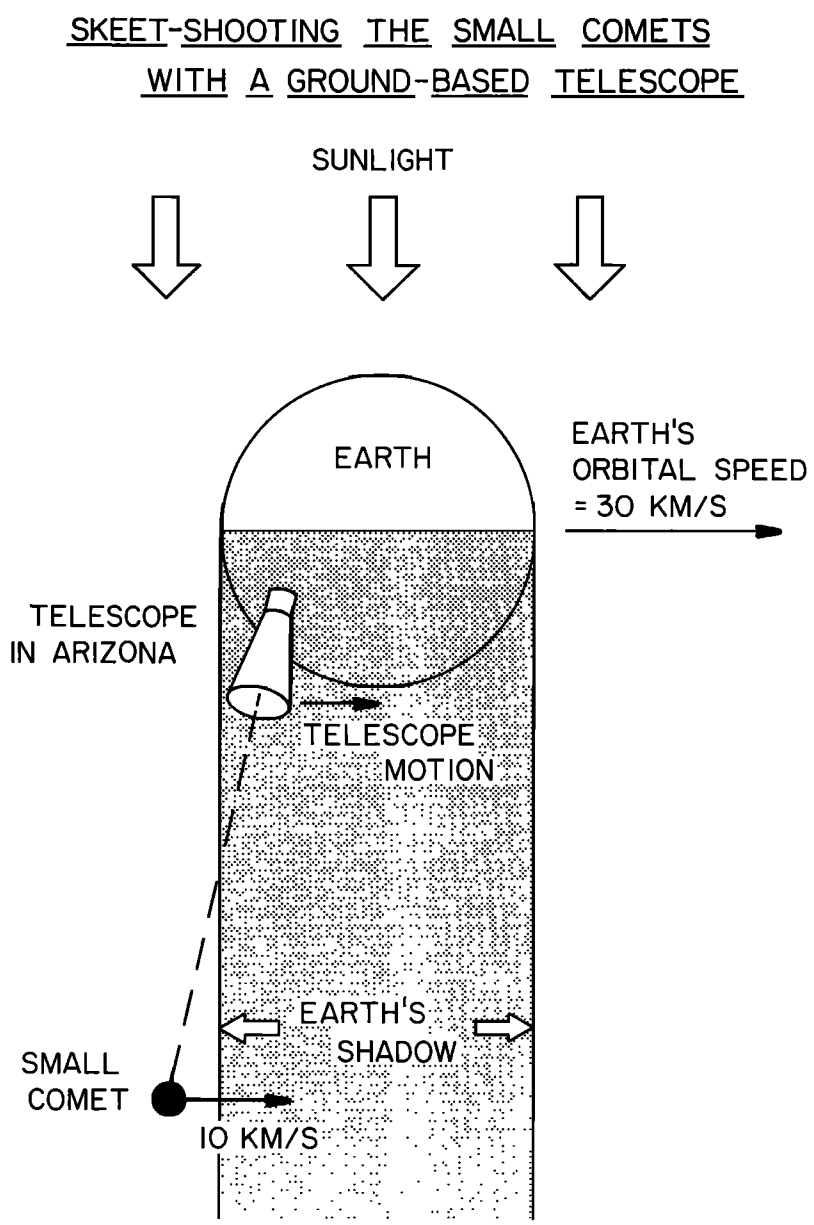

Figure 1. Viewing geometry for the "skeet-shooting" search mode for small comets with a ground-based telescope. The purpose of this operational mode is to lock onto the small comets in their prograde motion past the Earth at 10 km/s in order to maximize the dwell time of their images on a small number of pixels of the telescope's array sensor. This maximization of the dwell time allows the small-comet trail to be detected in the presence of skyglow and thermal noise of the sensor.

will not be able to record the presence of the small comets because of their rapid apparent motion across its image plane. Thus it is necessary to move the telescope's field of view so that the image of the small comet dwells at nearly the same location in the image plane during the image exposure time. This is called the "skeet-shooting" mode of observing the small comets [*Yeates,* 1989; *Sigwarth,* 1989; *Frank et al.,* 1990]. The distance from the telescope to a small comet which has no apparent motion on the image is called the "tuning distance." In practice, there will be some apparent motion of the small comet's image. The observable length of this trail in the image is limited by the apparent visual brightness of the small comet. In general, the length of the trail is less than 100 pixels because for longer trails the signal in the trail is overwhelmed by the noise due to readout noise of the CCD, thermal currents in the pixels of this sensor, and nighttime sky glow. The viewing of the small comets is conducted with tuning distances just outside of Earth's shadow in order to minimize

the Sun-comet-telescope angle, i.e., the solar phase angle, and thus to maximize the brightness of the comets.

The "window of opportunity" for observing the small comets is dependent upon the capabilities of a given telescope. For example, the search with the Spacewatch Telescope was conducted with the direction of its field of view at rest with respect to Earth's surface. That is, the drives which normally pointed the telescope in a fixed direction on the celestial sphere were shut off during the accumulation of an image. The telescope's field of view thus moved across the celestial sphere at the sidereal rate of 72.9 μrad/s and was pointed in directions generally parallel to the ecliptic plane. The tuning distance was 137,000 km. For trails with a length of up to 15 pixels, the radial range was 123,000 to 155,000 km. This range and the field of view of 0.04 deg^2 for the telescope define a detection volume for the small comets of about 7.6×10^{18} cm^3, or only about 0.7% of Earth's volume. The overall efficiency for detection within this volume is further decreased because the trails of some of the small comets exceed the maximum detectable length of 15 pixels. The calculation of this detection volume is presented at the end of this section.

Because the collecting area of the primary mirror for the IRO is significantly less than that for the Spacewatch Telescope, the window of opportunity is significantly different. That is, the detection of the small comets must be accomplished at closer distances to the Earth in order to compensate for this decreased sensitivity. The telescope's field of view must be moving approximately parallel to the ecliptic plane during the acquisition of an image. The azimuth-elevation drives of the IRO allowed the required flexibility for this operation. This is an important advantage with respect to the Spacewatch Telescope, which could provide only one tuning distance of 137,000 km. Indeed at this large range, and with its small mirror, the IRO is not capable of achieving detections of small comets. The tuning distance from the IRO to the small comets was typically in the range of about 45,000 to 50,000 km, with one series of observations at 89,000 km. Distances of 45,000 to 50,000 km are sufficiently close to the Earth to compensate for the smaller mirror relative to that of the Spacewatch Telescope. There was another important difference in the search modes for the two telescopes. The readout of images for the Spacewatch Telescope was sufficiently rapid that consecutive images of the same small comet were acquired. For the IRO the readout was too slow to acquire such image pairs, and a mechanical shutter was used to compensate by acquiring either two or three trails of the same small comet in a single frame as the comet's image moved across the CCD. For the acquisition of the two trails a 20-s exposure followed by a shutter-closed period of 10 s and a final 10-s exposure is used. Thus the first trail is twice as long as the second trail and allows determination of the direction of motion of the small comet. The acquisition of the three trails was the same as that for the two-trail images except that they were followed by a second 10-s period shutter closure and a third 10-s exposure for the small comet trail.

The operation of the IRO offered a significant advantage relative to that of the Spacewatch Telescope in eliminating the possibility that man-made Earth spacecraft were being detected in the images. The field of view of the Spacewatch Telescope was locked onto the sidereal rate which is the same as the apparent motion of geosynchronous spacecraft. Various factors were used to eliminate the possibility that spacecraft were being detected during the Spacewatch search [*Frank et al.*, 1990]. These earlier conclusions are now confirmed with the IRO observations. For example, for the worst case of a tuning distance of 89,000 km the motion of the IRO field of view at the geosynchronous radial distance of 42,000 km is 4.7 km/s in order to view a 10-km/s object at the tuning distance. The orbital motions of the spacecraft are 3.1 km/s. For the difference of 1.6 km/s the trail speed across the CCD is 7.9 arcsec/s, or 6.4 pixels/s, and the trail length during a 40-s image exposure is 256 pixels. This is the minimum trail length because the IRO is not scanning parallel to the geocentric equatorial plane. The minimum trail length is at least a factor of 4 greater than the observed trails of the small comets reported here. For the majority of the small-comet sightings the tuning distances were in the range of 45,000 to 50,000 km and the length of the spacecraft trails are in excess of 800 pixels. Although spacecraft angular speeds increase with decreasing geocentric radial position, the effective use of Earth's shadow eliminates detection of spacecraft at the lower altitudes.

The detection volume for the IRO is a strong function of the tuning distance R. For qualitative assessment the volume in configuration space can be estimated to vary as R^3. There is an additional factor of R^2 due to the fact that many of the trails will be too long for the recording of a definitive trail. Thus this rough, qualitative estimate of the dependence of detection volume with tuning distance is R^5.

This additional factor of R^2 can be qualitatively understood by consideration of the diagram in Figure 2. Consider the typical small-comet trajectory with perihelion at 1 AU, orbital inclination of 14.9° to the ecliptic plane, and a speed of 42.0 km/s in the Sun-referenced frame. When transformed into the Earth-referenced frame, this small comet will have a velocity of 15.3 km/s at an angle of 45° to the ecliptic plane. The component of velocity parallel to the ecliptic plane will be 10.8 km/s. Similarly, the component of velocity perpendicular to the ecliptic plane also will be 10.8 km/s. The IRO telescope is slewed nearly parallel to the ecliptic at a typical rate of 2.13×10^{-4} rad/s while accumulating the image. At a range from the telescope of 50,700 km the component of velocity parallel to the ecliptic plane will be matched exactly. However, this leaves the uncompensated component of ve-

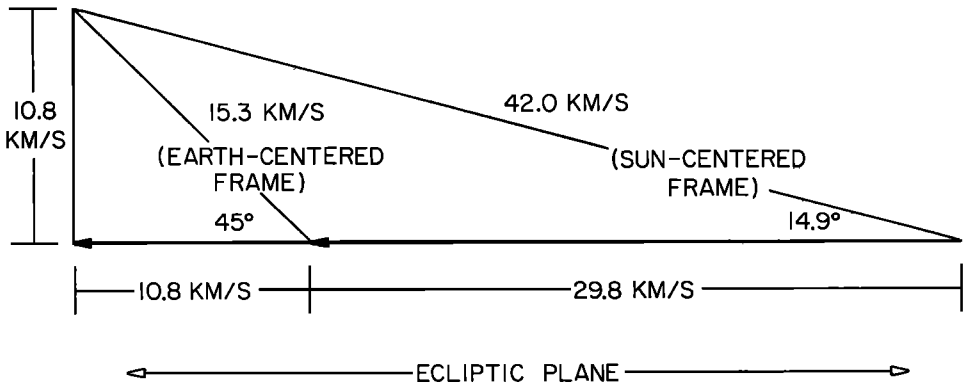

Figure 2. Diagram for the velocity of a small comet in the Sun-referenced and Earth-referenced frames. For this example the speed of the small comet is 42 km/s in the Sun-referenced frame with an inclination to the ecliptic plane of 14.9°. Note that motion of the field of view of the IRO telescope in a direction parallel to the ecliptic can cancel the apparent speed of the small comet in the direction parallel to the ecliptic. However, the uncompensated large component perpendicular to the ecliptic will not permit this telescope to detect this small comet.

locity perpendicular to the ecliptic plane of 10.8 km/s. For the range of 50,700 km from the telescope the length of the trail across the image acquired in 60 seconds with the IRO is (10.8 km/s/50,700 km) × (360 deg/2π) × (3600 arcsec/deg) × (1 pixel/1.23 arcsec) × (60 s) = 2140 pixels. Such a trail length is more than 20 times longer than that which can be detected with the IRO. Conversely, in order that this trail length is 100 pixels, then the angle of its motion relative to the ecliptic must be reduced to (100/2140) × (14.9°) = 0.7°. Thus a large fraction of the small comets within the physical volume sampled by the IRO are not seen.

A quantitative assessment of the detection volume is required in order to determine the fraction of the small comets which can be seen by the IRO as a function of tuning distance. Since both configuration space and velocity must be considered, essentially a phase space calculation is employed. The attributes of the small-comet orbits that are significant in the calculation of the effective search volume of the IRO are their prograde orbit around the Sun with perihelia near 1 AU and aphelia beyond the orbit of Jupiter, together with a maximum impact speed into Earth's atmosphere of 20 km/s [*Frank et al.*, 1986b]. These orbital parameters limit the velocity of the small comets with respect to the Sun-centered coordinate system to a range of about 39 to 42 km/s. The corresponding motions of the small comets in Earth's rest system are within a cone of half-angle 53° centered on the direction of Earth's orbital motion.

For the calculation of the effective detection volume of the IRO, the velocities of the small comets with respect to the Sun-centered coordinate system were assumed to be 40.6 km/s at 1 AU. The maximum trail length was set to 66 pixels for a total integration time of 40 s. The allowable range of solid angles was divided into 360 sections of width 1° in azimuth and 53 sections of width 1° in elevation for a total of 19,080 sectors. The number density of small comets per steradian was assumed to be constant. For each sector the direction and velocity for the small comets were determined. The maximum and minimum distances, R_{MAX} and R_{MIN}, respectively, for the detection of a small comet were computed for the condition that the maximum trail length was not exceeded. The detection volume for each of the above sectors was determined by $V(\theta, \varphi) = (\Omega/3)(R_{MAX}^3 - R_{MIN}^3)$, where Ω is the solid angle of the IRO field of view and θ, φ are the sector elevation, azimuth angles, respectively, from the direction of Earth's motion. The total effective detection volume for small comets was obtained by numerical integration of the sector volumes weighted with the appropriate spherical geometric factor and averaged over the full solid angle of 2.5 sr.

The effective detection volumes for the IRO as computed from the above rigorous numerical calculation are given in Table 1 for four tuning distances. For the full range of speeds of 39 to 42 km/s the variation of these effective volumes is ±30% of the values in Table 1 given for 40.6 km/s. It is obvious that a severe penalty in probability of detection is associated with an increase of apparent brightness by a decrease in the tuning distance. A similar calculation of the effective volume

Table 1. Effective Detection Volume for Small Comets

Tuning Distance, km	Effective Volume, m^3
47,000	2.0×10^{16}
68,000	1.2×10^{17}
89,000	4.7×10^{17}
137,000	4.1×10^{18}

for the Spacewatch Telescope detections of small comets in two consecutive images [*Frank et al.*, 1990] yields a value of 1.6×10^{18} m^3.

4. Determination of Random Trails

The observational campaign for the small-comet search was divided into two periods. During the first period the telescope was operated in the mode for acquisition of the same small comet as two trails in an image. The time span was October 19, 1998, through February 11, 1999. During the second period the operation of the telescope was changed in order to acquire three trails of the same comet in an image. This period was February 14, 1999, through May 1999, but the number of images acquired nightly after February 24 declined rapidly in order to accommodate student classroom work. A total of approximately 1500 usable images was acquired for the small-comet search with the number of images about equally divided between the above two periods.

A strong confirmation that the small-comet trails reported here were not due to random events is provided by the fact that no three-trail events were seen in the images which were acquired in the two-trail mode of telescope operation. And similarly, two-trail random events were not observed in the images when the telescope was operated in the three-trail mode.

The possibility that the trails are due to the clustering of bright pixel responses of the CCD sensor and hence not due to small-comet trails was investigated. Calculation of the autocorrelation function for pixels in an IRO image was used to demonstrate that the correlation of pixel responses in the vicinity of a given pixel was $\lesssim 5\%$ for views of the night sky glow without the presence of stars and small-comet trails. Thus the possibility of pixel clustering due to the CCD and/or electronics was eliminated.

It is important to further eliminate the possibility of random events with a rigorous analysis of the noise in the images. In order to characterize the occurrence of false trails due to the random fluctuations in the background responses of the CCD, a synthetic image of 512 × 512 pixels was created by a random draw from a normal distribution with a mean of 64 dn and a standard deviation of 17 dn. A Gaussian distribution provides an excellent fit to the distribution of readout responses of the IRO as shown in Figure 3. An automated computer search was performed on this synthetic image to locate the random trails with the highest signal-to-noise (S/N) ratios.

The search for random trails was begun by selecting a pixel at location (i0, j0) to serve as the exterior endpoint of the long trail, where i0 and j0 are integers between 1 and 512. The exterior point at location (i1, j1) of the short trail in the case of the two-trail telescope search or the exterior point of the second short trail in the case of the three-trail search was selected from an area of 101 × 101 pixels with corners (i − 50, j − 50) and (i + 50, j + 50) centered on the location (i0, j0). The minimum trail lengths allowed were 8 and 12 pixels for the two-trail and three-trail searches, respectively. These criteria required that a minimum of 1 pixel would be associated with each gap in the trail caused by closure of the shutter.

For the two potential random-trail endpoints, the pixels within each of the trail segments were identified. The trail width was assumed to be 5 pixels. A rectangle with horizontal and vertical sides was defined that surrounds the potential random trail. The corners of this rectangle surrounding the potential random trail were located at (minimum (i0, i1) − 5, minimum (j0, j1) − 5) and (maximum (i0, i1) + 5, maximum (j0, j1) + 5). This assures that the minimum border around the potential random trail within the rectangle is 2 pixels. The pixels that are in the rectangle and not in the trail are used to determine the mean and standard deviation.

The conditions for positive identification of a trail in the random image and in the images are highly constrained. The long trail is divided into two equal segments with total signals of S1 and S2. The signals in the short trails are S4 and S6. Of course, S6 is nonzero only for the three-trail search. The combined condition is met that S1 is within 1.0σ (standard deviation) of S2 and S2 is within 1.0σ of S1. S4 is within 1.0 σ of (S1 + S2)/2, and S6 is also within 1.0σ of (S1 + S2)/2. For the signals in the gaps, S3 and S5 are within 2.0σ of 0.0. In addition, the fraction of pixels with intensities >1.0σ must be ≥0.3 for each of the trail segments S1, S2, S4, and S6.

Each of the potential random-trail segments was tested in order to determine if the above trail criteria were met. If all of the trail criteria were satisfied, the characteristics of the random trail were tabulated. Random trails that overlap were compared and the random trail with the greater S/N was added to the table of random events, while the trail with the lesser S/N was discarded. It is important to note that this method compiled the table of random events which occurred at the highest S/N values for the random distribution. The distribution of these events in a plot of S versus S/N provided the envelope for which real events must substantially exceed. These plots are shown for each sighting of a small comet in the next section.

The synthetic image was searched systematically for all exterior short-trail endpoints within the 101 × 101 pixel square and for all exterior long-trail endpoints within the image. Each run required 3 weeks of time on a Digital Equipment Corporation Alpha server. The runs covered both the two-trail and three-trail searches and for average signals for each of the above trail segments S1, S2, S4, and S6 at average signals per pixel >0.2σ, 0.4σ, and 0.6σ.

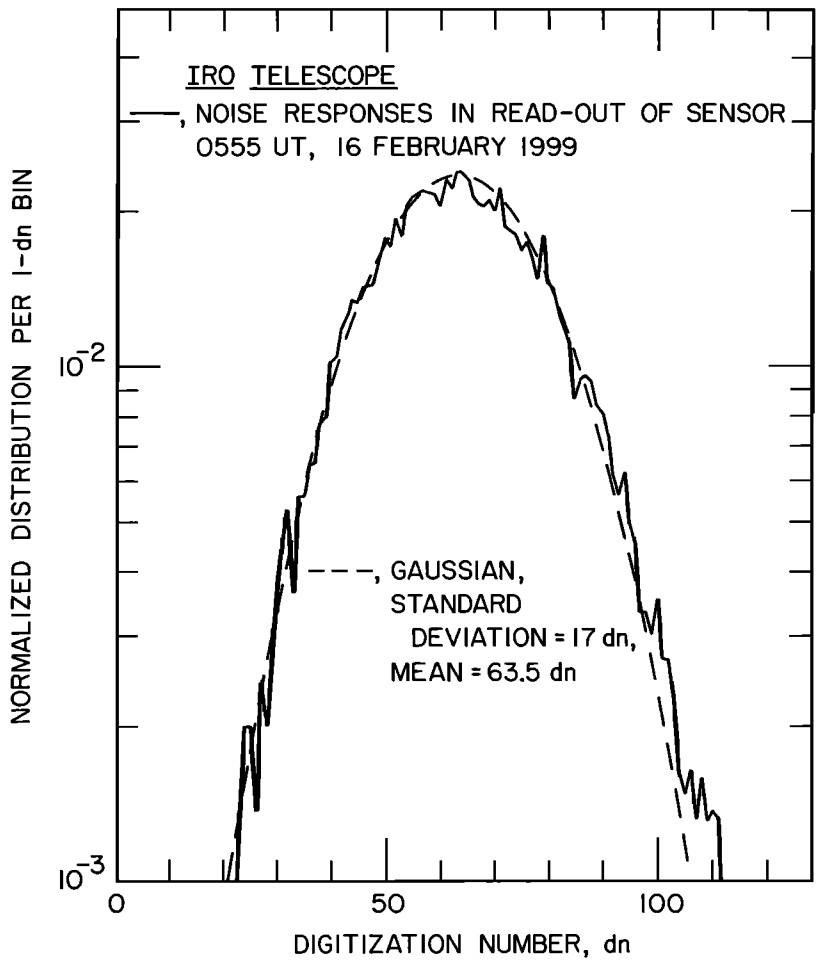

Figure 3. Noise responses for the readout of the IRO sensor when the telescope is viewing nighttime skyglow at 0555 UT on February 16, 1999. A total of 18,931 pixels is used for sections of the image with no star trails. The responses are well fit with a Gaussian with a mean of 63.5 dn and standard deviation of 17.0 dn. This well-behaved character of the noise distribution allows a rigorous calculation of the random occurrence rates of trails in the IRO images.

5. Observations

The observing campaign covered the new Moon periods during October 1998 through May 1999. Approximately 10 to 14 nights of observations centered on new Moon were the candidate periods, with the requirement that moonlight was not illuminating the atmosphere above the telescope. Many circumstances severely reduced the actual body of observations. These included atmospheric conditions such as rain, clouds, haze, and high winds. There were also malfunctions of the telescope such as those due to shutter failure, loose bolts, faulty software commands, and poor rejection of light from bright off-axis planets. A total of about 6000 images were taken for the small-comet search. They were carefully examined in order to identify the 1500 usable images. Nine sightings of small comets were identified in these images, a considerably lesser rate than obtained previously with the Spacewatch Telescope. This lower rate was anticipated owing to the closer tuning distances from Earth for the IRO as discussed in the previous section.

Images for two of the sightings of small comets are shown in Plates 1 and 2. The first sighting was obtained in the two-trail search mode (yellow box), and that in Plate 2, in the three-tail search mode; the times and dates of these sightings were 0622 UT on January 20, 1999, and 0555 UT on February 16, 1999, respectively. The actual images were arrays of 1024 × 1024 pixels, but because of the limitation of the computer screens used to photograph the above plates, an array of 997 × 884 pixels is displayed in Plate 1. Only about one fourth of an image is displayed in Plate 2 in order to exhibit the details of the three trails. Only a low-spatial-frequency third-order polynomial was used to flatten the responses of the pixels in the images. The application of the high-spatial-frequency filters which are available for these images invalidates our

rigorous determination of random trail characteristics and introduces further noise signals which essentially erase or highly degrade the comet trails. Hence no such filtering is used. The star trails in the above plates also have the same number of trail segments as those for the small comets, but their angular speed across the image due to the telescope motion across the celestial sphere produces trail sets with pixel lengths that exceed the dimensions of the images. The telescope motion is nearly tuned to that of these small comets across the sky. Their directions are not parallel to the direction of the star trails. The presence of the comet trails in Plates 1 and 2 is easily noted. The difficulty in the search lies in their infrequency of occurrence, about one in 150 images on the average, and eye fatigue after about 50 images or so in a viewing session.

The reader may also note that the left-hand member of the three-trail set in Plate 2 appears to be slightly out of line with those two trails to the right. This displacement is about 1 to 2 pixels and is due to the motion of the telescope field of view due to winds and the responses to the motor drives which are used for the telescope scans across the celestial sphere. Such effects are also seen in the star trails, for example, the slight dip in the star trail which ends near the upper center portion of Plate 2. For this and other reasons, the width of the small-comet trails used in our analysis is in the range of 4 to 8 pixels as given in Table 3. The widths of these small-comet trails are determined directly from the individual images. The lengths of each segment can be obtained by dividing the number of segment pixels in Table 2 by this trail full width given in Table 3.

The next step in the analysis is the quantitative verification that the small-comet trails satisfy the highly constrained set of requirements for a valid sighting as specified in section 4. The pixel responses for all nine small-comet sightings are given in Table 2. A few pixels which exhibit high responses because of ionization due to the passage of energetic charged particles or which are permanently flawed have been removed from the segment responses. Recall that segments 1 and 2 are the two halves of the long trail and segments 4 and 6 are the short trails. Segments 3 and 5 are the gaps between trails due to closing of the telescope's shutter. For each of these segments the number of pixels, the segment responses, and their 1σ values are given in Table 2. The reason that the gaps are shorter is due to the fact that the trails are lengthened from the overflow of responses due to the point spread function with half width of about 2 or 3 pixels. This effect is shown in the diagram of Figure 4. It is of value to note that this effect on the gaps for the Spacewatch Telescope observations is relatively small, since the trail accumulation time is 12 s for the first detection, a long gap time of 36 s as the image is read out, and followed by a 12-s accumulation time in the second image [*Frank et al.*, 1990]. The diameter of the blur circle for the Spacewatch Camera was about 2 pixels and thus considerably less than that for the IRO. In addition, it should be noted by the reader that some of the gap responses in Table 2 are negative because the mean background responses have been subtracted. For the small-comet sighting on October 19 to be valid, the segment responses 1 and 2, 413 and 430 dn, must be within 1σ of each other, the gap signal response 3 must be within 2σ of 0 dn, and the short-trail response 4, 518 dn, must be within 1σ of one half of the summed responses of segments 1 and 2, $(413 + 430)/2 = 422$ dn. The 1σ values are also given in Table 2, and the conditions for a valid set of two trails are well satisfied. This rigorous specification of sighted trails is necessary in order to determine the distribution of random trails in the images.

The distribution of detector noise is seen to be Gaussian to at least the 2σ level in Figure 3. At higher levels of sigma the frequency of pixels at these noise levels is sufficiently low that there will be no noise clusters at these brightnesses that would mimic a small-comet trail. The reader is reminded that the lengths and brightnesses of the small-comet trails in the images are highly constrained. The trails are not "single" pixel events. The detector response has not been "flat fielded" and is not required for this analysis. Small-scale fluctuations in the response of the detector were ruled out through an examination of the degree of correlation within clusters of pixels, rows, and columns.

The comparisons of the nine small-comet sightings and the distribution of random trails are shown in Figures 5 and 6. The total signals S are plotted as functions of S/N where N is the noise. The random events were calculated for three sets of average signals per pixel, 0.2σ, 0.4σ, and 0.6σ for both the two-trail and three-trail operational modes of the telescope. The table nearest to the average signal bucket for the detection of the small comet was used for the random events and the random signals S were normalized to the observed standard deviations in the pixel responses surrounding the small-comet trail. These average signals per pixel and the standard deviations are given in Table 3 for each sighting. The random events in Figures 5 and 6 define the envelope of maximum S and S/N for such trails. These values for the small comet sightings are well separated from the random events. It is of interest to note that visual examination of the test images does not identify any trails but that the computer-derived results must be used to find their location even for the longest and brightest of the false trails. On the other hand, the actual sightings are obvious in the images.

Inspection of Plates 1 and 2 may provide the reader with suggestions of other trails in these plates. However, the identification of a valid trail must be gained by quantitative evaluation of a

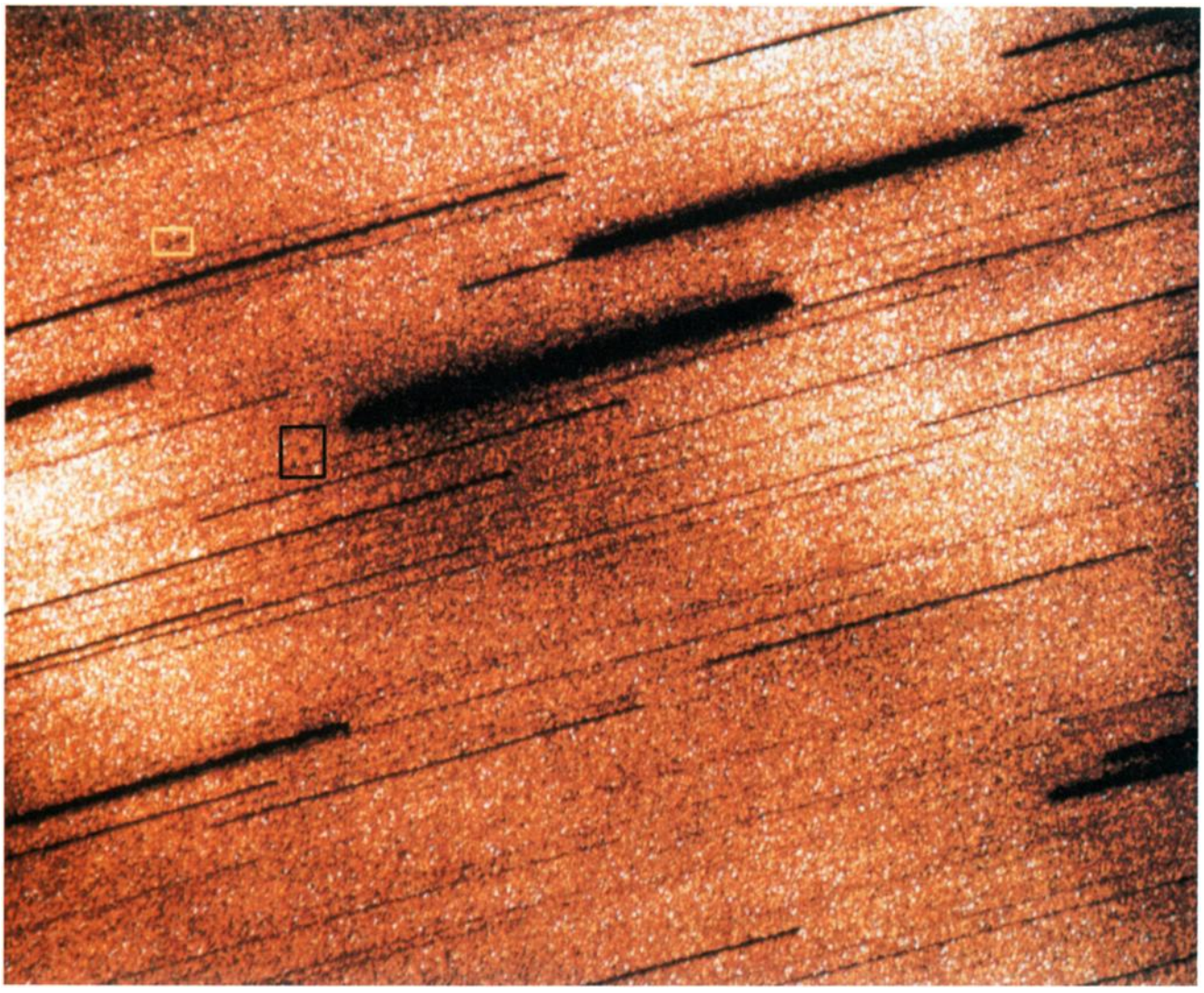

Plate 1. Image for the small-comet search taken at 0622 UT on January 20, 1999. Only a third-order polynomial flattening of the image responses was used to correct for large-scale gradients in order that all of the image could be displayed with a single color scale with a dynamic range sufficiently sensitive to reveal the small-comet trails. In practice, the small-comet trails are more easily searched for if the intensity scale is inverted such that the trails are dark. These photographs provide a reasonably accurate representation of the images as seen on a monitor screen during the image analyses. The trails of both relatively bright and dim stars due to the motion of the telescope's field of view across the celestial sphere are distributed across the image. The random fluctuations in the pixel responses provide the background seen across the entire image. The trails of a small comet as acquired in the two-trail search mode are indicated by the yellow box in the upper left-hand corner of the image. The long trail is on the right of the short trail. An expert referee identified a candidate three-trail event within the black box in the image. The failure of this event to satisfy the severe requirements for a real trail is summarized in Table 5.

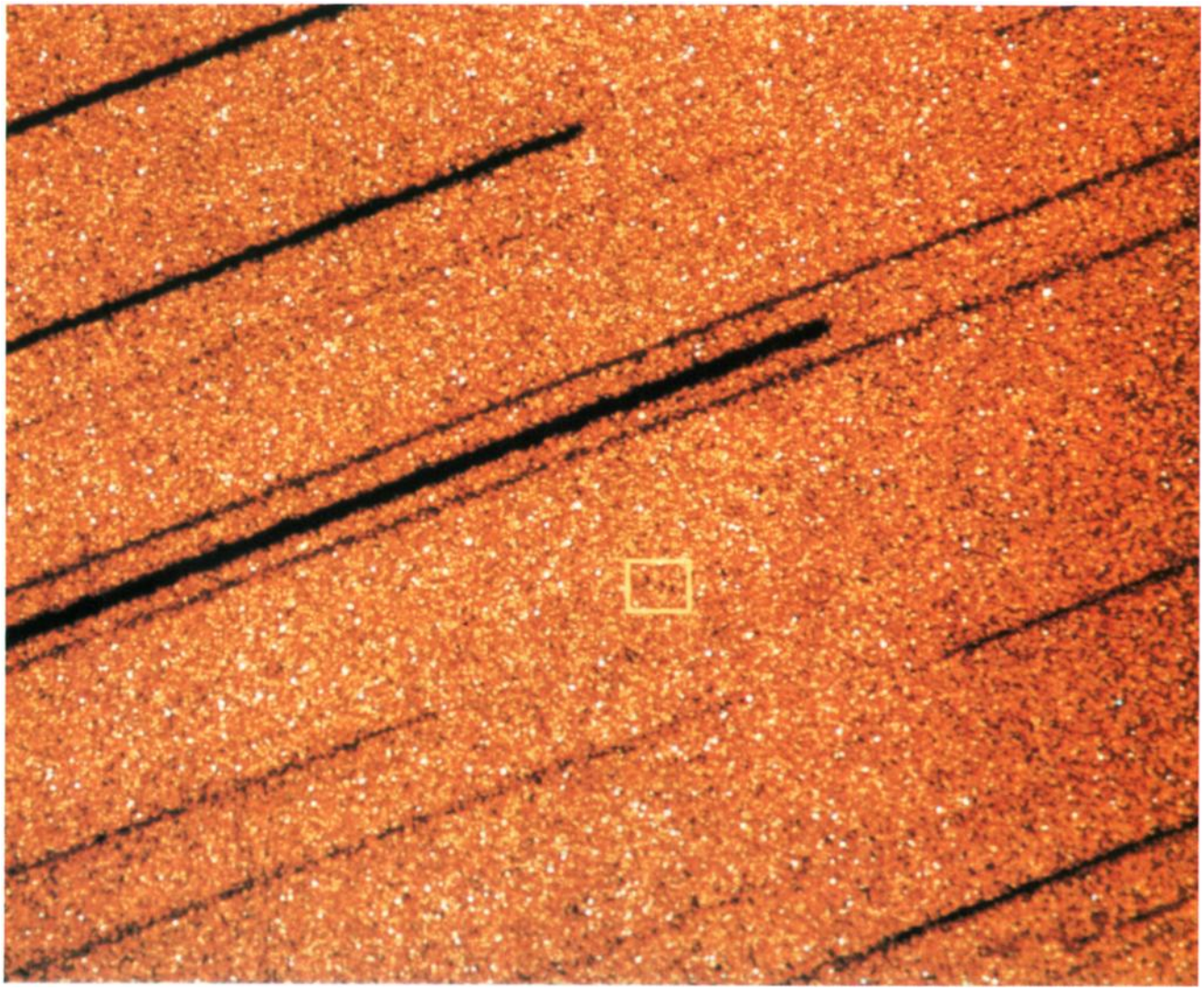

Plate 2. Continuation of Plate 1 for a small comet observed at 0555 UT on February 16, 1999. The three-trail search mode was used for the acquisition of this image. In order to display the details of the trails, only about one fourth of the entire IRO image is shown. The long trail is positioned on the left of the two short trails. The signals for each of the three trails are given in Table 2.

Table 2. Responses in Small-Comet Trails

	Segment					
	1	2	3	4	5	6
1, Oct. 19, 1998, 1043 UT						
No. pixels	74	73	48	82	0	0
Segment responses, dn	413	430	–100	518	0	0
1 σ	102	102	82	108	0	0
2, Oct. 28, 1998, 1011 UT						
No. pixels	82	82	67	87	0	0
Segment responses, dn	534	568	78	417	0	0
1 σ	141	141	128	145	0	0
3, Nov. 19, 1998, 0652 UT						
No. pixels	57	55	43	61	0	0
Segment responses, dn	465	497	187	547	0	0
1 σ	123	121	107	127	0	0
4, Nov. 20, 1998, 1002 UT						
No. pixels	74	76	41	85	0	0
Segment responses, dn	532	455	68	629	0	0
1 σ	133	135	99	143	0	0
5, Jan. 20, 1999, 0622 UT						
No. pixels	37	37	17	44	0	0
Segment responses, dn	347	324	45	320	0	0
1 σ	93	93	63	101	0	0
6, Jan. 21, 1999, 0658 UT						
No. pixels	83	83	71	87	0	0
Segment responses, dn	499	475	177	565	0	0
1 σ	140	140	130	144	0	0
7, Jan. 23, 1999, 0627 UT						
No. pixels	27	26	10	32	0	0
Segment responses, dn	387	265	–57	306	0	0
1 σ	83	82	51	90	0	0
8, Feb. 16, 1999, 0555 UT						
No. pixels	22	21	3	27	3	28
Segment responses, dn	221	281	–54	233	–0.4	180
1 σ	71	69	26	79	26	80
9, Feb. 16, 1999, 0649 UT						
No. pixels	63	63	47	68	48	68
Segment responses, dn	389	430	132	407	142	555
1 σ	140	140	121	146	123	146

candidate event, since visual impressions can be misleading. For example, we show the truth table in Table 4 for the two-trail event in Plate 1 (yellow box). All of the highly constrained requirements are satisfied. For the benefit of the reader, an expert referee recommended that a similar analysis be performed for a possible three-trail event in Plate 1 (black box). The evaluation is given in Table 5. The event severely fails the necessary requirements. For example, the S/N ratio of 3.5 is in the noise level of the images as to be noted in Figures 5 and 6.

Various parameters for the sightings of the small comets are given in Table 3, including trail lengths and widths, total signal S, tuning distance, and solar phase angle. Given for each sighting are the apparent visual magnitude V at the observing (tuning) distance and at 55,000 km and 137,000 km, where the latter was the value for the search with the Spacewatch Telescope. At a distance of 137,000 km the range of small-comet brightnesses reported here for the IRO search is 17.9^m to 20.0^m. The last three parameters in Table 3 were computed in order to assure that the tuning position

Table 3. Parameters for Detections of Small Comets With the Iowa Robotic Observatory

	Oct. 19, 1998	Oct. 28, 1998	Nov. 19, 1998	Nov. 20, 1998	Jan. 20, 1999	Jan. 21, 1999	Jan. 23, 1999	Feb. 16, 1999	Feb. 16, 1999
Time, UT	1043	1011	0652	1002	0622	0658	0627	0555	0649
Number of trails	2	2	2	2	2	2	2	3	3
Trail accumulation time, s	30	30	30	30	30	30	30	40	40
Total trail length, pixels	32	61	52	32	21	76	16	15	66
Trail full width, pixels	8	5	4	8	6	4	5	6	5
Signal S, dn	1361	1518	1509	1615	992	1539	959	915	1782
S/N	7.6	6.1	7.1	6.8	6.0	6.3	6.5	6.1	6.2
Standard deviation, dn	11.9	15.6	16.3	15.5	15.2	15.4	16.0	15.1	17.7
Average signal per pixel, dn (σ)	5.9 (0.50)	6.0 (0.39)	8.7 (0.53)	6.9 (0.44)	8.4 (0.55)	6.1 (0.39)	11.3 (0.70)	9.3 (0.62)	6.8 (0.38)
Tuning distance, km	89,010	50,760	45,820	50,340	45,250	44,900	45,200	47,700	46,230
Solar phase angle, deg	11.1	5.6	10.7	6.2	12.5	11.8	12.5	6.3	7.5
V at observing distance	17.0^m	16.9^m	16.9^m	16.8^m	17.3^m	16.9^m	17.4^m	17.7^m	17.0^m
V at 55,000 km	16.0^m	17.1^m	17.3^m	17.0^m	17.8^m	17.3^m	17.8^m	18.1^m	17.4^m
V at 137,000 km	17.9^m	19.0^m	19.3^m	19.0^m	19.8^m	19.3^m	19.8^m	20.0^m	19.4^m
Tuning radius,* km	22,200	9390	8380	9390	7850	8050	7870	8000	7660
Penumbral radius,* km	7230	6890	6850	6890	6840	6840	6840	6870	6860
Umbral radius,* km	5530	5870	5900	5870	5910	5910	5910	5890	5900

*Measured from the Earth-Sun line in the plane perpendicular to this line and through the tuning position.

Table 4. Truth Table for the Two-Trail Event in Plate 1 (All Requirements Must Be Satisfied)

Question					Response	
1. Small-comet trail is not parallel to star trails?					yes	
2. Small-comet trail does not intersect star trails?					yes	
3. Trail lengths sufficiently long for the appearance of gaps due to shutter closure?					yes	
4. S/N ≥ 6.0?					yes (6.0)	
5. Segment responses						
Segment number	1	2	3	4	5	6
Segment signal, dN	347	324	45	320	N/A	N/A
Standard deviation (σ)	93	93	63	101		
Pass test?	yes	yes	yes	yes		
6. Segment pixels						
Segment number	1	2	3	4	5	6
Number of pixels	37	37	17	44		
Fraction with ≥1σ responses	0.3	0.4	N/A	0.3		
Pass test?	yes	yes		yes		

was located in full sunlight and not in Earth's shadow. For example, the sighting on October 28 was 2500 km outside of the penumbra.

6. Summary and Discussion

We report here the results of a new survey of small comets with the Iowa Robotic Observatory which is located in the Sonoran desert near Sonoita, Arizona. This telescope is equipped with a primary mirror of 0.5-m diameter and a CCD sensor with an array of 1024 × 1024 pixels. The field of view is 0.35° × 0.35°. The observing campaign was conducted when there was no moonlight at the telescope's location during the period October 1998 through May 1999. A total of about 6000 images were taken, but maladies of the weather and the instrument operation reduced the usable set to about 1500 images.

The search mode was based on the skeet-shoot-

Table 5. Truth Table for Expert Referee's Selection of a Three-Trail Event in Plate 1 (All Requirements Must Be Satisfied)

Question					Response	
1. Small-comet trail is not parallel to star trails?					yes	
2. Small-comet trail does not intersect star trails?					no	
3. Trail lengths sufficiently long for the appearance of gaps due to shutter closure?					yes	
4. S/N ≥ 6.0?					no (3.5)	
5. Segment responses						
Segment number	1	2	3	4	5	6
Segment signal, dN	314	44	−64	215	82	198
Standard deviation (σ)	106	104	77	111	77	114
Pass test?	yes	no	yes	yes	yes	yes
6. Segment pixels						
Segment number	1	2	3	4	5	6
Number of pixels	48	46	25	53	25	55
Fraction with ≥1σ responses	0.3	0.2	N/A	0.2	N/A	0.2
Pass test?	yes	no		no		no

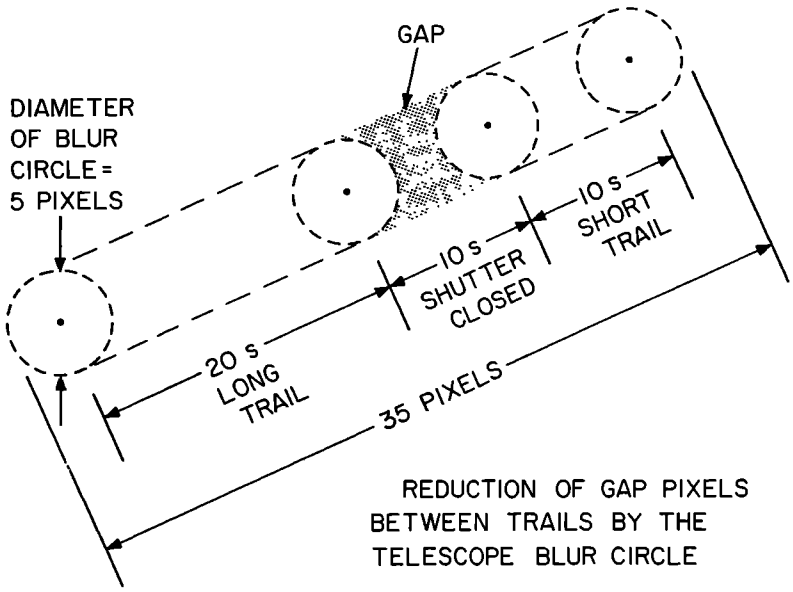

Figure 4. Diagram for the reduction of the numbers of darkened gap pixels due to the typical blur circle of the IRO telescope. For this example the total trail length is 35 pixels.

ing mode originally devised by *Yeates* [1989] in the search for small comets with the Spacewatch Telescope. That is, the pointing of the telescope is moved such that the image of a small comet is almost at rest with respect to the CCD pixel array. The range from the telescope to the small comet is designated as the tuning distance if the small comet is at rest in the CCD frame of reference. The small comets are moving in a stream with a speed of about 10 km/s with respect to Earth and generally directed parallel to the ecliptic plane [*Frank et al.*, 1986b; *Frank and Sigwarth*, 1993]. Of course, the apparent visual brightness of the small comets increases with decreasing tuning distance R. This brightness gain is accompanied by a severe decrease in the detection volume which varies approximately as R^5. The tuning distance for the Spacewatch Telescope was 137,000 km. Because the primary mirror of the IRO is significantly smaller, the tuning distance was also closer to Earth with a corresponding penalty in the volume for detection of the small comets. For the IRO search the tuning distances were in the range of about 45,000 to 50,000 km with a more limited series of images taken at 89,000 km on October 19, 1998.

In order to separate detection of the small comets from random events due to fluctuations of the pixel responses in the images, a shutter was used during the exposure of a single image. Two modes for the shutter were employed. The first mode was an exposure for 20 s, followed by a shutter-closed period of 10 s and ending with an exposure for 10 s. This mode provided the image of a small comet as two trails, the first trail twice as long as the second trail. The second mode employed the same sequence as the first mode but followed it with another shutter-closed period of 10 s and ending with another exposure for 10 s. This mode yielded three trails for a small comet, i.e., the first long trail followed by two short trails. The 1500 usable images were divided approximately equally between these two modes of operation.

The conditions for identification of the trails of the small comets were highly constrained by the demands on the characteristics of the trails and by their brightnesses. The separation of the small-comet trails from random events due to fluctuations of pixel responses in the images was verified in two ways. First, no three-trail events were found when the telescope was operated in the two-trail mode; similarly, no two-trail events were found when the telescope was gathering images in the three-trail mode. Second, further verification was provided by a rigorous statistical evaluation of the images which showed that the small-comet trails were characterized by signals S and signal-to-noise ratios (S/N) which greatly exceeded those for the random events in the images. These two verifications provide a high level of confidence in the detection of small comets.

Reference to the viewing geometry shown in the diagram of Figure 1 shows that Earth's shadow was used effectively in eliminating the possibility of the detection of man-made spacecraft and debris in orbit around Earth. For objects detected outside of this shadow, the angular speeds necessary to provide trails nearly at rest in the images are possible only with trajectories not bound by Earth's gravitational field.

A total of nine detections of small comets were recorded in the IRO images. Seven of these detec-

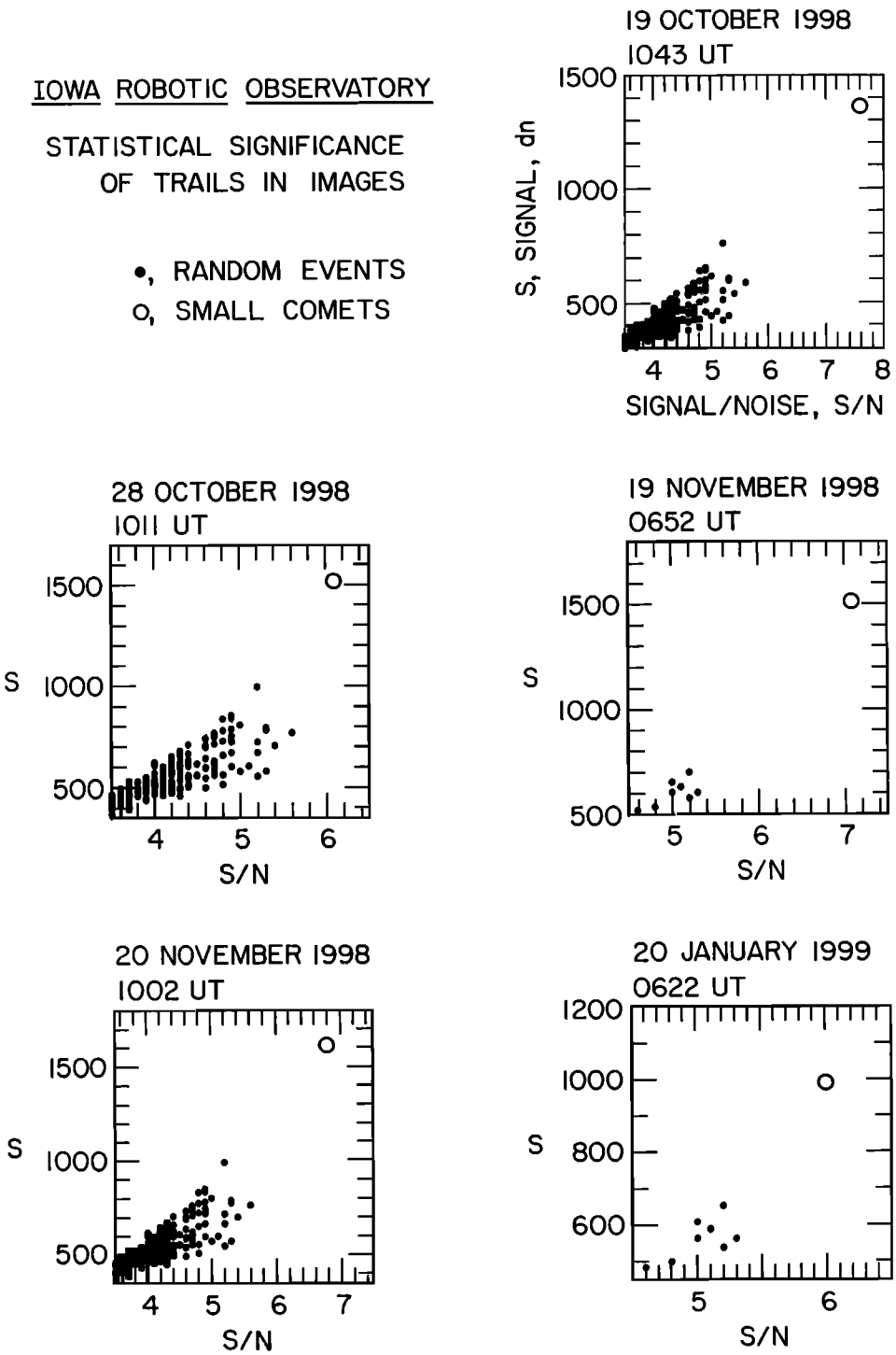

Figure 5. Signal S and the ratio of signal to noise (S/N) for five small-comet trails (open circles). The range of random trails for each of the five images is shown as small solid circles.

tions occurred during the period October 19, 1998, through February 11, 1999, when the telescope was operated in the two-trail mode. On and after February 14, 1999, the three-trail mode was used. This limited number of detections provides only a coarse estimate of occurrence rates, because the frequency of atmospheric holes as observed with both Dynamics Explorer 1 and the Polar spacecraft is higher during the months of October and November relative to the rates in January [*Frank and Sigwarth*, 1993, 1999].

The presently reported observations with the IRO can be placed in the perspective of those previously gained with the Spacewatch Telescope. The IRO detections are shown in Figure 7a as a function of visual magnitude V as normalized to

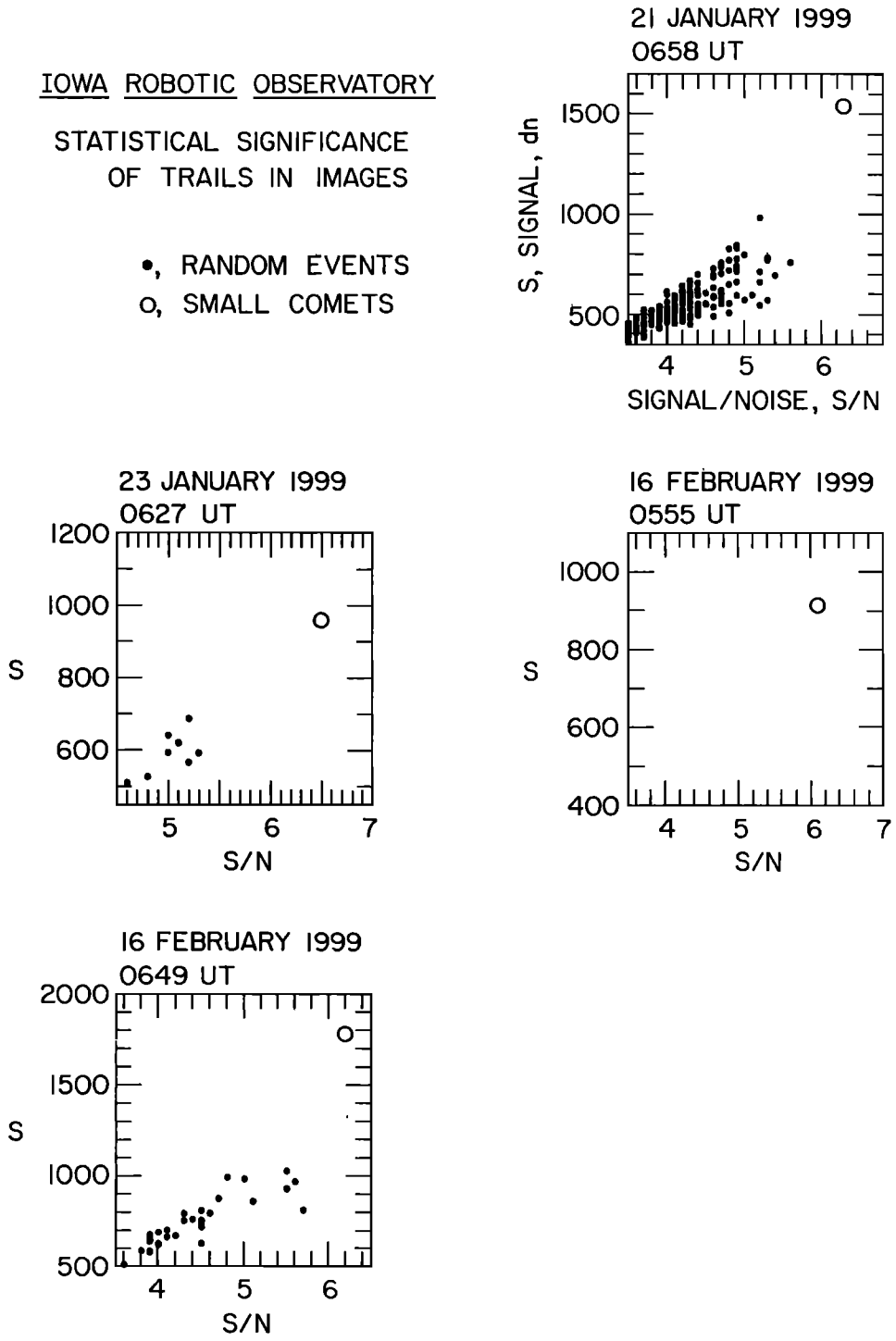

Figure 6. Continuation of Figure 5 for four small-comet trails.

the tuning range of 137,000 km with the Spacewatch Telescope. For comparison, the previous observations with the Spacewatch Telescope in single images [*Yeates,* 1989] and in two consecutive images [*Sigwarth,* 1989] are displayed in Figure 7b. The integral number densities of small comets with visual magnitude $\leq V$, in units of m^{-3}, are given as a function of V. The overall ranges of the small-comet brightnesses of the detections with the IRO and the Spacewatch Telescope are very similar.

The reader is reminded that *Yeates* [1989] reported the spatial densities of small comets in the brightness range of 19.1^m to 18.1^m. These integral densities with $<19.1^m$ were $\sim 10^{-19}/m^3$. Preliminary analysis of detections in two consecutive images in the brightness range of 19.3^m to 18.4^m provided similar spatial densities [*Frank et al.,* 1990]. Detailed analysis of the two consecutive image sets extended the brightness range down to $\sim 19.6^m$ with an increase of the integral densities to

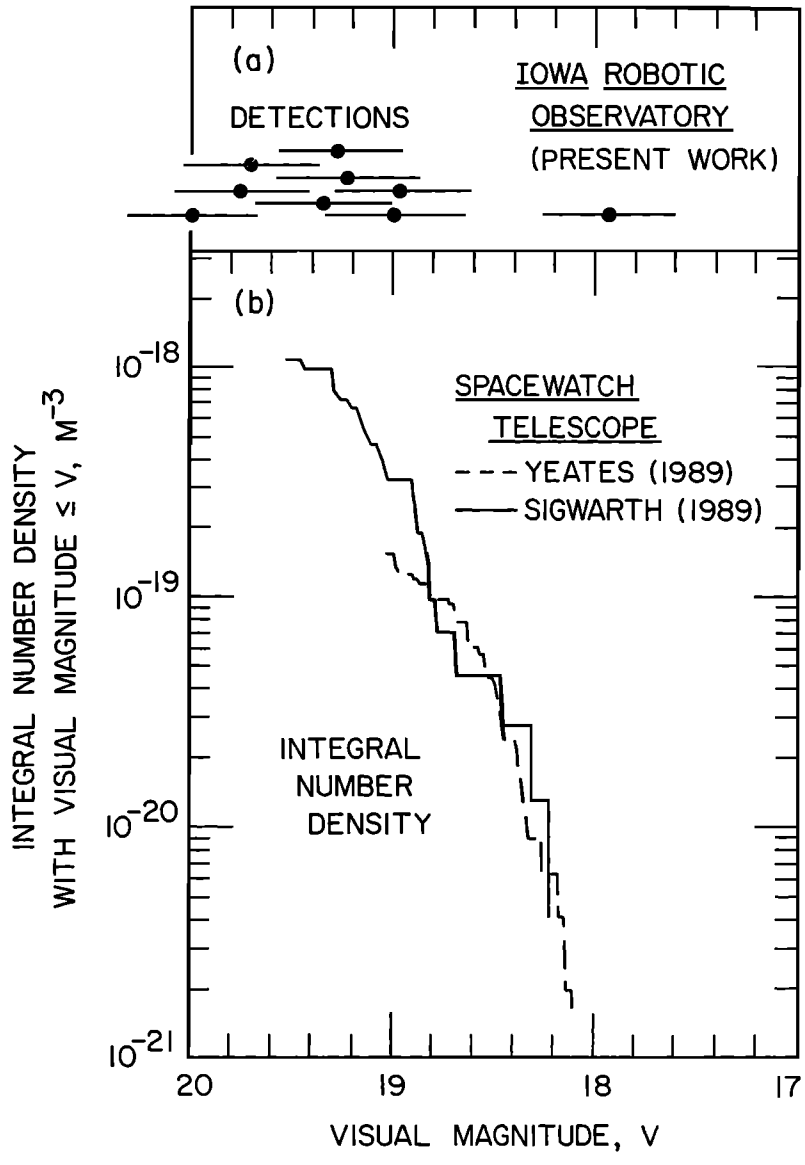

Figure 7. (a) Detections of small comets with the Iowa Robotic Observatory as functions of apparent visual magnitude V during October 1998 through February 1999. The estimated uncertainties in the brightnesses of the small comets are given as horizontal error bars. The visual magnitudes are given for the Spacewatch Telescope range of 137,000 km. (b) Integral number densities of small comets with visual magnitudes $\leq V$ for two series of observations with the Spacewatch Telescope. The first series was taken on November 20 and 21, 1987, and on January 23, 1988 [*Yeates,* 1989]. The small comets were each recorded in a single image. The sightings of 33 small comets were reported. The second series of observations were taken on April 19, 1988, for two consecutive images of the same small comet [*Sigwarth,* 1989]. There were 25 sightings of small comets in 48 such pairs of images.

$\sim 10^{-18}/m^3$ [*Sigwarth,* 1989]. As was pointed out by *Frank and Sigwarth* [1993] with their Figure 12, the brightness range $\lesssim 19^m$ corresponds to masses which are sufficiently large to yield atmospheric holes in the images of the upper atmosphere with Dynamics Explorer 1. These interplanetary densities of $\sim 10^{-19}/m^3$ are sufficient to account for the average global occurrence rates of the atmospheric holes.

For values of assumed mass densities, reflectances, and phase laws for the small comets, their total masses have been computed for the Spacewatch Telescope observations by *Frank and Sigwarth* [1993]. Although there are large uncertainties for the values of the above parameters, a mass of about 2×10^7 g is in the midrange of the estimates.

The effective detection volumes given in Table 1 can be used to estimate the frequency of small-comet trails in the IRO images. First note that this volume for the IRO at a tuning distance of 47,000 km is a factor of 200 smaller than the IRO

volume at the Spacewatch tuning distance of 137,000 km. However, the smaller primary mirror of the IRO is unable to detect the small comets at this distance, and the penalty is a decrease in detection volume in order to increase their brightness. Inspection of Figure 7b finds that the integral number density is about 10^{-18} /m^3 at visual magnitudes $V \leq 19.6^m$. The IRO detection volume is about 2×10^{16} m^3, which is reduced to 10^{16} m^3 because about one half of the field of view is lost on the average owing to the large number of star trails. The actual tuning distance and V for each of the nine sightings of small comets are given in Table 3. The computed brightnesses V for the tuning distance for the Spacewatch Telescope are also given in Table 3 and plotted in the summary shown in Figure 7a. The number of small-comet sightings which are expected for the 1500 usable images from the IRO on the basis of the previous observations from the Spacewatch Telescope is then $(1500) \times (10^{16}\ \text{m}^3) \times (10^{-18}\ /\text{m}^3) = 15$. The observed number of sightings with the IRO for $V \leq 20.0^m$ is 9, in good agreement with the previous Spacewatch sightings within the counting statistics of the limited number of events. The reader should note in Figure 7b that the spatial densities of small comets are much less for $V \leq 18.2^m$, i.e., $\sim 3 \times 10^{-21}$ /m^3. Thus a set of 33,000 IRO images for a tuning distance of 47,000 km is required for one detection, on the average. There was one IRO detection of a relatively bright small comet at $V = 18.0^m$ as shown in Figure 7a. However, this sighting was acquired at a tuning distance of 89,000 km, where the detection volume has increased to 2.4×10^{17} m^3. For the set of 100 usable images at this tuning distance the sighting was fortuitous with a probability of success of about 0.1. The reader should note that at this larger tuning distance of 89,000 km, small comets with V in the range of 20.0^m to 19.0^m cannot be reliably detected because of the low responses of the IRO telescope.

Although the number of small-comet detections are limited for this IRO survey, it can be concluded that the spatial densities of the small comets are in agreement, within factors of 2 to 3, with those previously obtained with the Spacewatch Telescope.

7. Brief Summary of Optical Searches for Small Comets

The first optical detections of the small comets were successfully acquired with the Spacewatch Telescope at Kitt Peak in Arizona [*Yeates,* 1989; *Sigwarth,* 1989; *Frank et al.,* 1990]. Descriptions of this telescope have been published *[Gehrels et al.,* 1986, 1987]. By coincidence, this telescope was sufficiently sensitive to detect the small comets by shutting off the telescope drives which are normally used to view in a direction which is fixed in relation to the celestial sphere. The purpose in shutting off these drives is to increase the dwell time of the image of the small comet on the pixels of the telescope's sensor. The corresponding detection distance for the small comets was about 137,000 km from Earth.

Our present successful detection of the small comets with the Iowa Robotic Observatory located near Sonoita, Arizona, was possible because of the programmable elevation and azimuth drives for its field of view. The small aperture of this "student telescope" demanded that its field of view be moved approximately parallel to the ecliptic plane in order to capture the small comets which are moving in a stream at about 10 km/s relative to the reference frame of Earth. This target distance is in the range of 50,000 km in order to adequately increase the apparent brightness of the small comets. These searches were possible owing to the fact that the small comets are moving in a well-organized stream past Earth and not in random directions and speeds.

Other telescopes have been investigated as to their capabilities for the detection of small comets. One of these is the telescope for the Near-Earth Asteroid Tracking (NEAT) Program which is located on the summit of the Haleakala volcano crater in Hawaii [*Pravdo et al.,* 1999]. This special camera for searching for near-Earth asteroids is mounted on a U.S. Air Force telescope which is used for monitoring Earth-orbiting spacecraft and debris. When the telescope drive is shut off in order to track the small comets, the limiting magnitude is 17.8^m, which is about 0.8^m brighter than the Spacewatch threshold (D. L. Rabinowitz and E. F. Helin, private communication, 1998). The Spacewatch threshold brightness is shown in Figure 7b of the present paper. If these researchers are able to reprogram the telescope drives in a manner similar to that used for the smaller-aperture IRO, then the small comets should be easily sighted by the NEAT telescope.

The Hubble Space Telescope is well known as one of the "crown jewels" of optical astronomy. Numerous discussions with Ralph Bohlin of the Space Telescope Science Institute (STScI) in Baltimore, Maryland, were directed toward the possibility that this telescope be used for a small-comet search. These discussions culminated in a presentation of the search requirements at STScI on March 24, 1998. The search would employ the Wide Field and Planetary Camera 2 [*Burrows et al.,* 1994; *Trauger et al.,* 1994]. The Hubble spacecraft would be continuously rotated such that the small comets would be detected at a range of about 1,000,000 km. In October, when the small-comet fluxes are greatest at Earth, the detection rate would be such that a sufficient number of small-comet sightings would be gained in a 30- to 60-min period. There was one drawback for this exciting search because there was no tested operational software which allowed the acquisition of images at the required relatively high spacecraft rotation rates. It was generally agreed that the optical search be conducted by ground-based telescopes

rather than risking the health of the Hubble Space Telescope.

Recently, there was a report that a new search for the small comets has been conducted with a much improved Spacewatch Telescope [*Harris and Scotti,* 1998]. A total of 17 image frames were reported to have been acquired. There is considerable interest among several scientists in examining these images. R. A. Hoffman of the Goddard Space Flight Center, who is chair of an informal committee with the purpose of encouraging observations which are relevant to the small-comet search, has made several requests that the images be made available to interested scientists without success.

Our own immediate interest is to obtain the collaborative support and participation of several astronomers in gaining access to a telescope with sufficient aperture to use a series of filters while a small comet is in view in order to determine its spectral characteristics.

Acknowledgments. The authors are indebted to Gregory L. Pickett, senior research engineer in the Department of Physics and Astronomy at The University of Iowa, for donating the hundreds of hours required for the tedious examination of the images taken with the Iowa Robotic Observatory. We benefited from the substantial comments and suggestions of the three referees. This research was supported in part by discretionary funding from the university and by NASA contract NAS5-30316 and NASA grants NAG5-3328 and NAG5-7712.

Janet G. Luhmann thanks Hyron Spinrad and two other referees for their assistance in evaluating this paper.

References

Burrows, C. J., M. Clampin, R. E. Griffiths, J. Krist, and J. W. MacKenty, *Wide Field and Planetary Camera 2 Instrument Handbook,* edited by C. J. Burrows, Space Telesc. Sci. Inst., Baltimore, Md., May 1994.

Dessler, A. J., The small comet hypothesis, *Rev. Geophys., 29,* 355-382, 1991.

Frank, L. A., and J. B. Sigwarth, Atmospheric holes and small comets, *Rev. Geophys., 31,* 1-28, 1993.

Frank, L. A., and J. B. Sigwarth, Detection of atomic oxygen trails of small comets in the vicinity of Earth, *Geophys. Res. Lett., 24,* 2431-2434, 1997a.

Frank, L. A., and J. B. Sigwarth, Trails of OH emissions from small comets near Earth, *Geophys. Res. Lett., 24,* 2435-2438, 1997b.

Frank, L. A., and J. B. Sigwarth, Atmospheric holes: Instrumental and geophysical effects, *J. Geophys. Res., 104,* 115-141, 1999.

Frank, L. A., J. B. Sigwarth, and J. D. Craven, On the influx of small comets into the Earth's upper atmosphere, I, Observations, *Geophys. Res. Lett., 13,* 303-306, 1986a.

Frank, L. A., J. B. Sigwarth, and J. D. Craven, On the influx of small comets into the Earth's upper atmosphere, II, Interpretation, *Geophys. Res. Lett., 13,* 307-310, 1986b.

Frank, L. A., J. B. Sigwarth, and C. M. Yeates, A search for small solar system bodies near the Earth using a ground-based telescope: Technique and observations, *Astron. Astrophys., 228,* 522-530, 1990.

Gehrels, T., B. G. Marsden, R. S. McMillan, and J. V. Scotti, Astrometry with a scanning CCD, *Astron. J., 91,* 1242-1243, 1986.

Gehrels, T., J. D. Drummond, and N. A. Levenson, The absence of satellites of asteroids, *Icarus, 70,* 257-263, 1987.

Harris, A. W., and J. V. Scotti, On the optical detectability of mini-comets (abstract), *Eos Trans. AGU, 79*(17), Spring Meet. Suppl., S236, 1998.

Pravdo, S. H., et al., The Near-Earth Asteroid Tracking (NEAT) program: An automated system for telescope control, wide-field imaging, and object detection, *Astron. J., 117,* 1616-1633, 1999.

Sigwarth, J. B., A search for small comets in consecutive images acquired with a ground-based telescope, Ph.D. thesis, Univ. of Iowa, Iowa City, 1989.

Trauger, J. T., et al., The on-orbit performance of WFPC2, *Astrophys. J., 435*(1), L3-L6, 1994.

Yeates, C. M., Initial findings from a telescopic search for small comets near Earth, *Planet. Space Sci., 37,* 1185-1196, 1989.

L. A. Frank and J. B. Sigwarth, Department of Physics and Astronomy, 212 Van Allen Hall, University of Iowa, Iowa City, IA 52242–1479. (louis-frank@uiowa.edu; john-sigwarth@uiowa.edu)

(Received February 22, 2000; revised August 10, 2000; accepted August 11, 2000.)